

# Diffusion-limited-aggregation on a directed small world network

Jie Ren<sup>1</sup>, Wen-Xu Wang<sup>2</sup>, Gang Yan<sup>3</sup>, and Bing-Hong Wang<sup>2\*</sup>

<sup>1</sup>*Department of Physics,*

<sup>2</sup>*Department of Modern Physics,*

<sup>3</sup>*Department of Electronic Science and Technology,  
University of Science and Technology of China,  
Hefei, 230026, PR China*

(Dated: August 22, 2018)

For real world systems, nonuniform medium is ubiquitous. Therefore, we investigate the diffusion-limited-aggregation process on a two dimensional directed small-world network instead of regular lattice. The network structure is established by rewiring connections on the two dimensional directed lattice. Those rewired edges are controlled by two parameters  $\theta$  and  $m$ , which characterize the spatial length and the density of the long-range connections, respectively. Simulations show that there exists a maximum value of the fractal dimension when  $\theta$  equals zero. Interestingly, we find that the symmetry of the aggregation pattern is broken when rewired connections are long enough, which may be an explanation for the formation of asymmetrical fractal in nature. Then, we perform multifractal analysis on the patterns further.

PACS numbers:

## I. INTRODUCTION

Nonequilibrium growth models leading naturally to self-organized fractal patterns, the structure of which strongly depends on the dynamics of the growth process, are of continuing interest due to their relevance for many important fields[1]. Diffusion-limited -aggregation (DLA)[2] is probably the most remarkable growth model for pattern formation. This model generates complex and mysterious fractal structures[3, 4], which seem to be generated as well in natural systems in which growth is controlled by diffusive, including dielectric breakdown[5], electrochemical deposition[6], colloid aggregation[7], film growth[8], viscous fingering[9], Laplacian flow[10] etc.

In the original DLA model[2], particles released at a point distant from the cluster execute random walks until they find a nearest neighbor site of the cluster and irreversibly stick at this site. However, for many physical processes, the medium is nonuniform so that the probability of jumping from site  $i$  to site  $j$  is usually not equal to that from  $j$  to  $i$ . Moreover, except nearest-neighbor jumps, there also exist some nonlocal jumps through which the particle can move to a distant site at a step. One example is the diffusion of adatoms on metal surfaces, in which the long jumps play a dominating role[11, 12]. A bunch of defects or impurities in the substrate may also play the part of the long-jump path in the case of weak adsorbate-substrate interaction[13], which is important for the thin-film growth, heterogeneous catalysis, and oxidation. Hence, the traditional undirected regular lattice will miss important information of medium and it is unconformity to characterize the actual DLA process. This thus calls for the use of

network structure with directed long-range connections.

On the other hand, complex networks have recently attracted an increasing interest among physicists[14, 15, 16]. In particular, small-world (SW) networks, introduced by Watts and Strogatz[17], have been extensively studied because they constitute an interesting attempt to translate the complex topology of social, biological, and physical networks into a simple model. Two dimensional (2D) SW networks result from randomly rewiring a fraction of links of a 2D regular lattice. Several dynamical models have recently been studied in order to understand the effect of SW topology on classical systems such as the Ising model[18], the spread of epidemics[19], aggregation[20], random walks[21], etc. Such models are expected to capture the essential features of the complicated processes taking place on real networks.

In this paper, we investigate the DLA process on a 2D directed SW network, in which the directed links correspond to the directed irreversibly jumps and the node is regarded as the lattice point of the real space, respectively.

## II. THE MODEL

In order to construct the directed SW network, we start from a 2D square lattice of size  $L \times L$  consisting of sites linked to their four nearest neighbors by both outgoing and incoming links, as shown in Fig. 1. Then, we reconnect nearest-neighbor outgoing links to a different site chosen at random with the probability

$$p(r) \sim e^{-\theta r}, \quad (1)$$

where  $r$  is the lattice distance between the two selected sites and  $\theta(\theta \in [-1, 1])$  is the clustering exponent which characterizes the localized degree of the long-range links in the lattice. The formula corresponds to the diffusiv-

---

\*Electronic address: bhwang@ustc.edu.cn

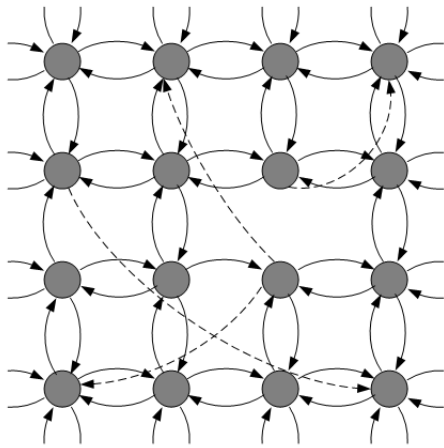


FIG. 1: Sketch map of a directed 2D SW lattice. Dotted lines represent rewired connections. Arrows indicate the direction of the corresponding connection.

ity represented by Arrhenius relation as usual in surface science[11, 12, 13]. The reconstructing process is repeated until  $m$ , the number of long-range rewiring connections, reaches a desired value. Note that by performing this procedure every site will have exactly four fixed outgoing links and a random number of incoming links. When the clustering exponent  $\theta=0$ , we have a uniform distribution over long-range connections, and the present model reduces to the basic 2D directed SW network[22]. As  $\theta \rightarrow 1$  ( $\theta \rightarrow 1$  denotes  $\theta$  tends to 1), the long-range links of a site become more and more local in its vicinity. In reverse, as  $\theta \rightarrow -1$ , the long-range rewiring outgoing links are in favor of the farther sites. Thus, the clustering exponent  $\theta$  serves as a structural parameter controlling the spatial length of the long-range connections.

Based on the directed 2D SW network as constructed above, we have performed extensive numerical simulations for the DLA with size of the reconstructed lattice  $L=1000$  with number of particles  $N=10000$ . Starting from an immobile seed at the center of the lattice, a particle is released at a random position where it departs from the outer radius of the growing pattern. Then the particle jumps along the direction from the current site to one of its linked sites which are not occupied by the growing pattern, with equal probability step by step. At last, the particle irreversibly sticks at the nearest neighbor site of the growing pattern in terms of the physical distance and the pattern will grow gradually. To reduce the effect of fluctuation, the calculated result is taken average over 10 different network realizations and 10 independent runs for each network configuration for each set of parameters  $(\theta, m)$ .

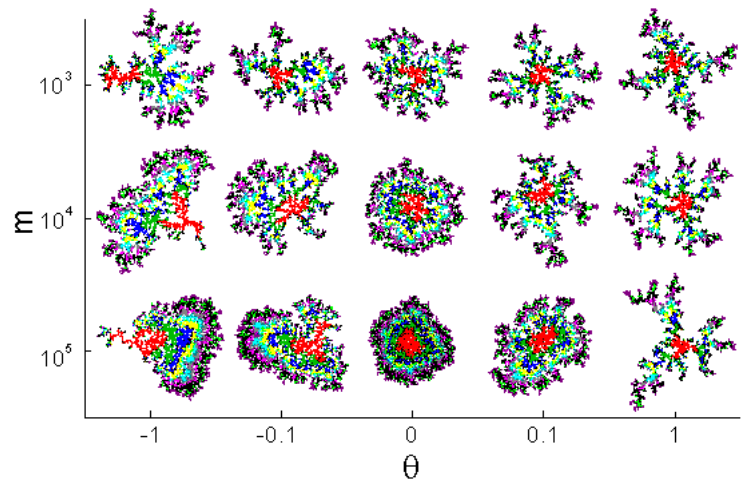


FIG. 2: The simulation patterns as a function of the clustering exponent for the number of long-range connections  $m=1000$ , 10000 and 100000 respectively. Each color represents 1000 particles in order.

### III. SIMULATION RESULT AND DISCUSSION

Fig 2 illustrates the patterns of DLA which exhibit rich behaviors for different parameters  $\theta$  and  $m$ . For each  $\theta$ , it can be seen that with the increase of  $m$  the patterns of DLA become thicker and denser, however, which is not obvious for large  $\theta$ , approximately 1. For each  $m$ , the pattern is nearly the most dense when  $\theta=0$ . While, it gets thin and sparse when  $\theta$  departs from 0 tending to 1 or  $-1$ . However, it is astonishing that the symmetry of the aggregation pattern is markedly broken while  $\theta < 0$ , which is more obvious as  $\theta$  tends to  $-1$ . To quantify the patterns of DLA, we calculate the fractal dimensions  $D_0$  of the DLA by box-counting method[3, 4], which are shown in Fig. 3. It is clear that there exists a maximum value of  $D_0$  when  $\theta$  equals 0 for each  $m$ . It can be seen that the more  $\theta$  departs from 0, the more  $D_0$  decreases. Moreover, it is found that  $D_0$  decreases more fast when  $\theta \rightarrow 1$  than  $\theta \rightarrow -1$ .

It is well-known that the special randomly branching, open structure of a DLA pattern results from the effects of screening, which is manifested through the fact that the tips of most advanced branches capture the incoming diffusing particles most effectively. In the present work, due to the long-range connections, particles can jump directly to distant sites, including the traditionally completely screened deep fjord. The nonlocal connections effectively weaken the screening effect so that the pattern of aggregate becomes compact and the fractal dimension  $D_0$  increases with  $m$  increasing. On the other hand, the clustering exponent  $\theta$ , which restricts the spatial length of the long-range connection, affects the morphology of the aggregate and the fractal dimension  $D_0$ . As  $\theta \rightarrow 1$ , the long-range links are restricted more and more local in its vicinity so that the capacity of weakening the screen-

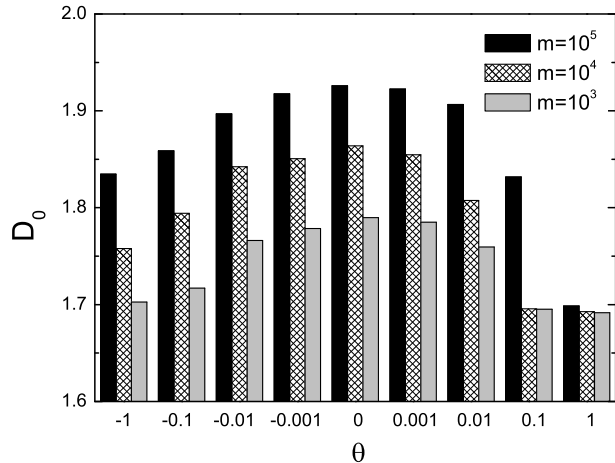


FIG. 3: The fractal dimension  $D_0$  of patterns as a function of the clustering exponent  $\theta$  for several  $m$ .

ing effect vanishes gradually. Finally,  $D_0$  does not vary and the morphology of the aggregate seems like the original DLA pattern, as shown in Fig. 2 and Fig. 3. When  $\theta=0$ , the spatial lengths of the long-range connections are entire random, neither too distant nor too local and they have a uniform distribution. Then, due to intensive weakening for the screening effect, the random particle has the chance to appear on arbitrary sites on the underlying network so that the pattern becomes thick and compact, corresponding to increase of  $D_0$ . However, as  $\theta \rightarrow -1$ , the long-range links tend to the sites as distant as possible and the irreversible jumps along directed links break the symmetry of dynamics. Thus, small fluctuations are enhanced, and this instability together with the randomness inherent in the model leads to a complex asymmetrical behavior.

However, the fractal dimension  $D_0$  is a rough description because the pattern becomes asymmetric while  $\theta \rightarrow -1$ . So, we have performed the multifractal analyse[23, 24] here to see more details. It should be noted that our measurements concern the pattern itself other than its harmonic measure[25].

Further characterization of the DLA patterns can be achieved by determining the generalized fractal dimensions  $D_q$ . Cover the pattern with a grid of square boxes of size  $\varepsilon$  and define  $P_i(\varepsilon)$  to be the relative portion of the pattern in cell  $i$ , and define  $N(\varepsilon)$  to be the total number of boxes of size  $\varepsilon$  needed to cover the whole pattern. The relative portion  $P_i(\varepsilon)$  can be described as multifractal as:

$$P_i(\varepsilon) \sim \varepsilon^\alpha, \quad (2)$$

$$N_\alpha(\varepsilon) \sim \varepsilon^{-f(\alpha)}, \quad (3)$$

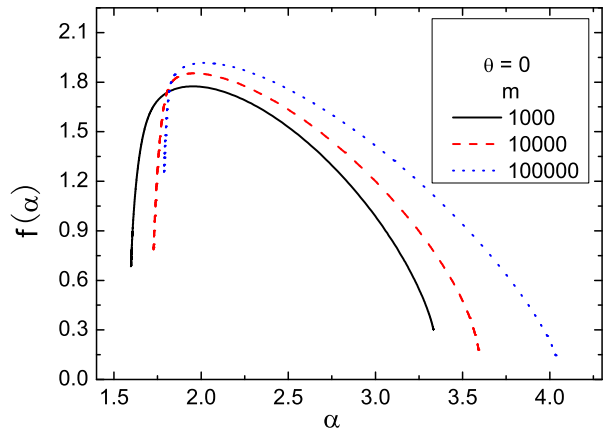


FIG. 4: The multifractal spectra  $f(\alpha)$  of the distribution of the patterns, with various number of long-range connections,  $m=1000, 10000, 100000$ , respectively.

where  $\alpha$  is the singularity,  $N_\alpha(\varepsilon)$  the number of small squares of relative size  $\varepsilon$  with the same singularity, and  $f(\alpha)$  is the fractal dimension.

To describe quantitatively the subtle geometrical feature of the pattern, the fractal dimension  $f(\alpha)$  can be obtain from the partition function  $\chi_q$ :

$$\chi_q = \sum_i^{N(\varepsilon)} P_i^q(\varepsilon), \quad (4)$$

and its power law of  $\varepsilon$ ,

$$\tau_q = \lim_{\varepsilon \rightarrow 0} \frac{\ln \chi_q}{\ln \varepsilon}, \quad (5)$$

where  $q$  is the moment order and  $\tau_q$  the index of the power law. The generalized fractal dimension is defined as:

$$D_q = \frac{\tau_q}{q-1}, \quad (6)$$

Then,  $(\alpha, f(\alpha))$  can be obtained from  $(q, D_q)$  by performing the Legendre transformation:

$$\alpha = \frac{d}{dq} [(q-1)D_q], \quad (7)$$

$$f(\alpha) = \alpha q - (q-1)D_q, \quad (8)$$

In our calculation, the moment order  $q$  is taken for -30 to 30.

We have calculated the multifractal spectra  $f(\alpha)$  of the distribution of the patterns, with various number of long-range connections,  $m=1000, 10000, 100000$ , respectively, for a original directed 2D SW lattice,  $\theta=0$ . Figure

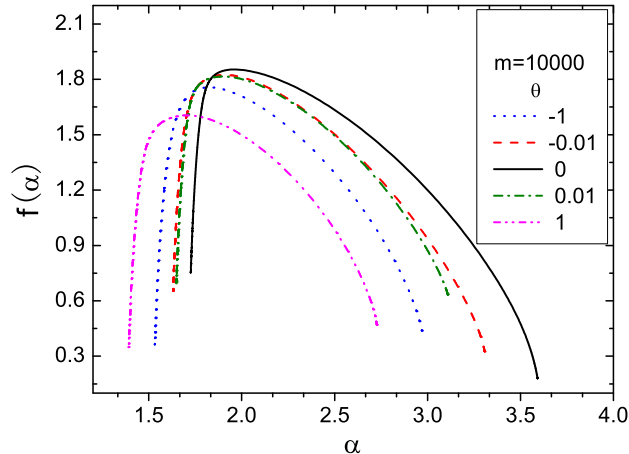


FIG. 5: The multifractal spectra with several value of the cluster exponent  $\theta$ , -1, -0.01, 0, 0.01, 1, for  $m=10000$ .

4 shows the result. It can be seen that the curve becomes higher and the range of singularity  $\alpha$  becomes wider with increasing the number of the long-range connections. In Table I, the multifractal parameters of the distribution are listed. The multifractal spectrum can be used to provide more information about the subtle geometrical difference, because of the  $\alpha_{max}$  and  $\alpha_{min}$  connecting with the smallest probability and the largest probability of the spatial distribution [show by Eq.(2)]. The result (Table I) show that  $\alpha_{max}$  and  $\alpha_{min}$  both increase with increasing  $m$ , while  $\Delta\alpha = \alpha_{max} - \alpha_{min}$  also increases, indicating that the pattern becomes less irregular, less nonuniform, and more dense. Moreover, Fig. 5 illustrates that the multifractal curves with several value of the cluster exponent  $\theta$ , -1, -0.01, 0, 0.01, 1, for a directed 2D SW lattice,  $m=10000$ . More quantitative details can be seen in Table II. It illustrates that the range of  $\alpha$  is the broadest and the curve is the maximal when  $\theta=0$ , suggesting the pattern is the most dense, compact and regular, which corresponds to Fig. 2 and Fig. 3 showed above.

TABLE I: Some multifractal parameters of Figure 4.

$m$	1000	10000	100000
$\alpha_{min}$	1.598	1.726	1.786
$\alpha_{max}$	3.332	3.591	4.034
$\Delta\alpha = \alpha_{max} - \alpha_{min}$	1.734	1.865	2.248
$f(\alpha_{min})$	0.684	0.752	1.251
$f(\alpha_{max})$	0.303	0.180	0.147
$\Delta f = f(\alpha_{min}) - f(\alpha_{max})$	0.381	0.572	1.104

- [1] P. Meakin, *Fractal, Scaling and Growth far from Equilibrium* (Cambridge University Press, Cambridge, U.K.,1998).  
 [2] T.A. Witten and L.M. Sander, Phys. Rev. Lett. **47**, 1400 (1981).

TABLE II: Some multifractal parameters of Figure 5.

$\theta$	-1	-0.01	0	0.01	1
$\alpha_{min}$	1.532	1.630	1.726	1.648	1.392
$\alpha_{max}$	2.969	3.307	3.591	3.109	2.727
$\Delta\alpha = \alpha_{max} - \alpha_{min}$	1.437	1.677	1.865	1.461	1.335
$f(\alpha_{min})$	0.352	0.652	0.752	0.676	0.347
$f(\alpha_{max})$	0.438	0.326	0.180	0.635	0.470
$\Delta f = f(\alpha_{min}) - f(\alpha_{max})$	-0.086	0.326	0.572	0.041	-0.123

#### IV. CONCLUSION

In summarize, we have investigated the DLA process on a nonuniform medium which is characterized by a directed 2D SW lattice with two introduced parameters ( $\theta, m$ ) which govern the style of the pattern. It is found that as  $m$  increases, the aggregation pattern become thicker and denser, which indicates the fractal dimension increases. We also figure out that there exists a maximum value of  $D_0$  in the case of  $\theta = 0$  for any value of  $m$ , which implies the densest aggregation pattern corresponds to the cases of entire randomly length of long-range connections, neither too long nor too local. Interestingly, we find that the symmetry of the aggregation pattern is broken when rewired connections are long enough. The directed long-range links contribute to the formation of asymmetrical patterns. The random walk of the particles along the directed links is irreversible so that the principle of detailed balance is broken. Hence, the asymmetry of the dynamics finally results in the asymmetry patterns. To give detailed description of the asymmetrical pattern, we have performed multifractal analysis on the patterns. The subtle geometrical difference among these patterns for different parameter value can be provided by the multifractal parameters. Although the model we have proposed is very simple, the simulation results demonstrate that it can capture most of the general features of asymmetrical growth processes. Other than the traditional asymmetrical factor such as gravity, magnetic field, electric field, etc, the asymmetrical factor of our model is the directed link, which causes the break of dynamics symmetry inherent. It may be an new explanation for the formation of asymmetrical fractal behavior in nature.

- [3] T. Vicsek, *Fractal Growth Phenomena* (World Scientific, (Singapore, 1992).  
 [4] A.-L. Barabasi and H. E. Stanley, *Fractal Concepts on Surface Growth* (Cambridge University Press, Cambridge, UK, 1995).

- [5] L. Niemeyer, L. Pietronero, and H. J. Wiesmann, Phys. Rev. Lett. **52**, 1033 (1984).
- [6] R. M. Brady and R. C. Ball, Nature (London) **309**, 225 (1984); M. Matsushita, M. Sano, Y. Hayakawa, H. Honjo and Y. Sawada, Phys. Rev. Lett. **53**, 286 (1984).
- [7] M. Kolb, R. Botet, and R. Jullien, Phys. Rev. Lett. **51**, 1123 (1983).
- [8] W. T. Elam, S. A. Wolf, J. Sprague, D. U. Gubser, D. Van Vechten, G. L. Barz, and P. Meakin, Phys. Rev. Lett. **54**, 701 (1985).
- [9] K. J. Måløy, J. Feder, and T. Jøssang, Phys. Rev. Lett. **55**, 2688 (1985).
- [10] L. Paterson, Phys. Rev. Lett. **52**, 1621 (1984).
- [11] D. C. Senft and G. Ehrlich, Phys. Rev. Lett. **74**, 274 (1995).
- [12] T. R. Linderoth, S. Horch, E. Lægsgaard, I. Stensgaard, and F. Besenbacher, Phys. Rev. Lett. **78**, 4978 (1997).
- [13] M. Schunack, T. R. Linderoth, F. Rosei, E. Lægsgaard, I. Stensgaard, and F. Besenbacher, Phys. Rev. Lett. **88**, 156102 (2002).
- [14] R. Albert and A.-L. Barabási, Rev. Mod. Phys. **74**, 47 (2002).
- [15] S. N. Dorogovtsev and J. F. F. Mendes, Adv. Phys. **51**, 1079 (2002).
- [16] M. E. J. Newman, SIAM Review **45**, 167 (2003).
- [17] D. J. Watts and S. H. Strogatz, Nature (London) **393**, 440 (1998); S. H. Strogatz, *ibid.* **410**, 268 (2001).
- [18] A. Barrat and M. Weigt, Eur. Phys. J. B **13**, 547 (2000).
- [19] R. Pastor-Satorras and A. Vespignani, Phys. Rev. Lett. **86**, 3200 (2001).
- [20] S.-Y. Huang, X.-W. Zou, Z.-G. Shao, Z.-J. Tan, and Z.-Z. Jin, Phys. Rev. E **69**, 067104 (2004).
- [21] J. D. Noh, and H. Rieger, Phys. Rev. Lett. **92**, 118701 (2004).
- [22] A. D. Sánchez, J. M. López, and M. A. Rodríguez, Phys. Rev. Lett. **88**, 048701 (2002).
- [23] H. G. E. Hentschel and I. Procaccia, Physica D **8**, 435 (1983).
- [24] T. C. Halsey, M. H. Jensen, L. P. Kadanoff, I. Procaccia, and B. I. Shraiman, Phys. Rev. A **33**, 1141 (1986).
- [25] O. Praud and H. L. Swinney, Phys. Rev. E **72**, 011406 (2005).